2016-04-11

Folded Meandered Monopole for Emerging Smart Metering & M2M Applications in the Lower UHF Band Primary tabs

Abraham Loutridis
Technological University Dublin

Matthias John
Trinity College Dublin, matthias.john@tudublin.ie

Max Ammann
Technological University Dublin, max.ammann@tudublin.ie

Recommended Citation

Loutridis, A., John, M., & Ammann, M. J. (2016) Folded Meandered Monopole for Emerging Smart Metering & M2M Applications in the Lower UHF Band, *IEEE Antennas & Propagation Magazine,* vol. 58, no. 2, pp. 60-65, 2016.

Funder: SFI

Folded Meandered Monopole for Emerging Smart Metering & M2M Applications in the Lower UHF Band

A. Loutridis, *Student Member, IEEE*, M. John, *Member, IEEE* and, M.J. Ammann, *Senior Member, IEEE*

***Abstract*— A compact folded meander-line monopole for smart metering and M2M applications is presented. It operates over a tunable frequency range of 412-475 MHz. The miniaturization is based on a double-sided meandering structure and the rear positioning of the feeding and shorting strips. A sliding via connector is used for tuning. The proposed antenna is compact 15 mm ($0.02\lambda_0$) × 42.3 mm ($0.058\lambda_0$), low cost and easily fabricated. A 21-24% total-efficiency was provided across the tunable band. Installed performance was evaluated in a meter housing placed on a concrete wall. Measured and simulated results are provided.**

***Index Terms*—Meander-line, Monopole Antenna, M2M, Smart Meters**

I. Introduction

IN the last decade, the requirement to modernize the electric grid infrastructure to incorporate decentralized energy production and renewable sources has re-established grid operators as Distribution System Operators [1]. This is driving increased demand for smart meters, sensors and intelligent switches with integrated wireless communication capability. Smart meters are typical Machine-to-Machine communication devices (M2M) and apply cellular communications technologies [2]. Flexibility and low operational cost are the main reasons for the new radio technology to play a significant role in the connectivity of smart metering and smart grid devices.

The 450 MHz band for terrestrial mobile and fixed communication covering 410–470 MHz spectrum [3] is attractive for in-building penetration. Automated meter reading systems are allocated narrowband channels in this band. CDMA and more recently eLTE operate in this band with channel bandwidths in the region of ~1-5 MHz.

One of the advantages of 450 MHz is that it uses larger cells than GSM (900 MHz) or 3G (1920–2190 MHz) and provides coverage of a larger number of smart metering or smart grid devices (lowest number of base stations per area covered).

As antenna sizes for M2M and smart meter technologies decrease due to constraints on available space, the performance becomes more challenging at the lower UHF frequencies in a dimensional trade-off. At this early stage of smart meter technologies, there are few reported works on embedded antennas in the 450 MHz band. However, there are a variety of techniques used to reduce monopole size, including folding [4] and normal mode helical techniques [5], but these are not appropriate for integration in packaging. In [4, 5] the antenna efficiency is not reported and in [5] the antenna covers a -10 dB S_{11} bandwidth of 40 MHz. Lumped elements and diode varactors are also used to improve matching, bandwidth and control the resonant frequency, but can increase cost and decrease antenna efficiency to 3% and the gain to -12 dBi [6]. In [7] the antenna is located on a 230 mm × 130 mm ground plane with a reported efficiency of 25% at 470 MHz .The gain is not reported. In [8, 9], high permittivity ceramic is used to reduce the antenna size, but these antennas are limited by smaller bandwidth and surface wave excitation which leads to lower radiation efficiency.

In both [8, 9] the antenna efficiency is not reported and the antennas are located on a large ground plane size (230 mm × 130 mm). In [8] only the simulated gain (-7.5 dBi) is given, while in [9] the gain is less than -9 dBi. In [10] the $51 \times 28\ \text{mm}^2$ antenna provides a -10 dB S_{11} bandwidth of 4.5 MHz at 433 MHz with a -13 dBi gain. The efficiency is not reported.

In this paper a folded meander-line monopole antenna for emerging smart metering and M2M applications is presented. The low-cost, easy to manufacture compact antenna is low-profile, easy to package and provides omnidirectional radiation characteristics with excellent total-efficiency, given its size.

The performance is not heavily dependent on the ground plane (130 mm × 70 mm) size and the operating frequency can be easily tuned with the sliding via for the installed performance. A 21% - 24% total-efficiency is provided across the tunable band.

II. Antenna Design

The antenna, shown in Fig. 1, is printed on 1.5 mm double-sided FR-4 substrate ($\varepsilon_r = 4.3$, $\tan\delta = 0.025$) with copper thickness of 0.035 mm. The antenna of height $h = 15\ \text{mm} \approx 0.02\lambda_0$ and length $l = 42.3\ \text{mm} \approx 0.058\lambda_0$ is located on the corner of a rectangular ground plane of

Manuscript received May 29, 2015. This publication has emanated from research conducted with the financial support of Science Foundation Ireland (SFI) and is co-funded under the European Regional Development Fund under Grant Number 13/RC/2077.

A. Loutridis and M.J. Ammann, are with the Antenna & High Frequency Research Centre, Dublin Institute of Technology, Dublin 8, Ireland (e-mail: abraham.loutridis@mydit.ie; max.ammann@dit.ie).

M. John is with CTVR - the Telecommunication Research Centre, Trinity College Dublin, Dublin 2, Ireland (e-mail: johnm@tcd.ie).

dimension 130 mm × 70 mm. The FR-4 ground plane represents a typical device PCB. The feeding and shorting strips (width = 0.5 mm, 0.7 mm respectively) are located on the rear side of the substrate and connected to the meander line (width = 0.5 mm) on the front side using a via and a slider.

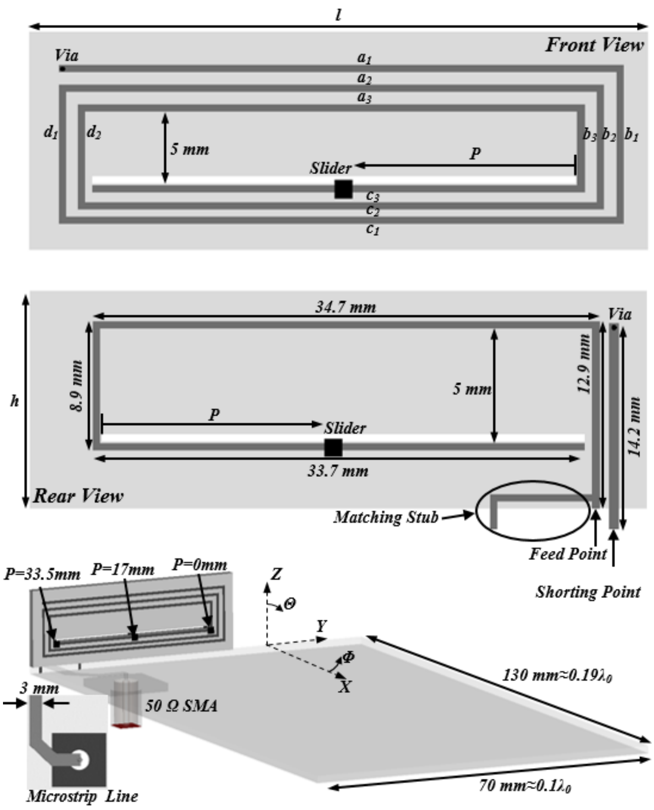

Fig. 1. Meandered folded monopole antenna on a typical device ground plane.

The separation between the horizontal strips a_1, a_2 and a_3 is 0.85 mm. The gap between the vertical strips b_1, b_2 and b_3 is 0.83 mm. The lower horizontal strips c_1 and c_2 have a separation of 0.5 mm and between c_2 and c_3 the separation is 0.68 mm. The gap between the two vertical strips d_1 and d_2 is 0.8 mm. The separation between the strips was optimised to obtain the best impedance matching for the desired frequency. The length of the strips are listed in Table I.

The moveable U-shaped aluminum via-slider is mounted through a slot in the substrate, connecting the two sides of the PCB. This enables device turning for the CDMA450 and eLTE band use. The start and the end positions of the via-slider are at 0 mm ≤ P ≤ 35 mm (Fig. 1). The monopole antenna is fed using a 50 Ω microstrip line (width = 3 mm) with a SMA connector below the ground plane (Fig. 3).

TABLE I
STRIP LENGTH

Strip	Length (mm)
a_1	38.6
a_2	37.3
a_3	34.7
b_1	10.9
b_2	8.55
b_3	6
c_1	38.6
c_2	36
c_3	33.7
d_1	9.55
d_2	7.2

III. SIMULATED AND MEASURED RESULTS

A matching stub is added to control the performance and shifts downwards the resonant frequency by introducing additional capacitance and reducing the real impedance towards 50 Ω, as it shown in Fig. 2. The matching stub consists of two strips (width 0.5 mm) with horizontal and vertical length 7 mm and 2.5 mm, respectively. The matching stub is shorted to the ground plane.

The via-slider position, P can be pre-adjusted to provide tuning at any frequency across the band. Fig. 4 shows the measured and simulated S_{11} for 5 different tuning positions of the via-slider P, which controls the resonant frequency.

For $S_{11} \leq -10$ dB, the tunable range is 412.4-474.8 MHz (BW = 62.4 MHz) and for $S_{11} \leq -6$ dB the antenna provides a tuneable bandwidth of 71.6 MHz, i.e. (409.5–481.1 MHz). For the lowest centre-frequency of 414 MHz, λ_0 ~ 724.5 mm and the measured -6 dB and -10 dB bandwidths are ~8 MHz and ~3 MHz respectively. The length of the meander-line at the via-slider position P = 33.5 mm is 378 mm which is almost $\lambda_0/2$.

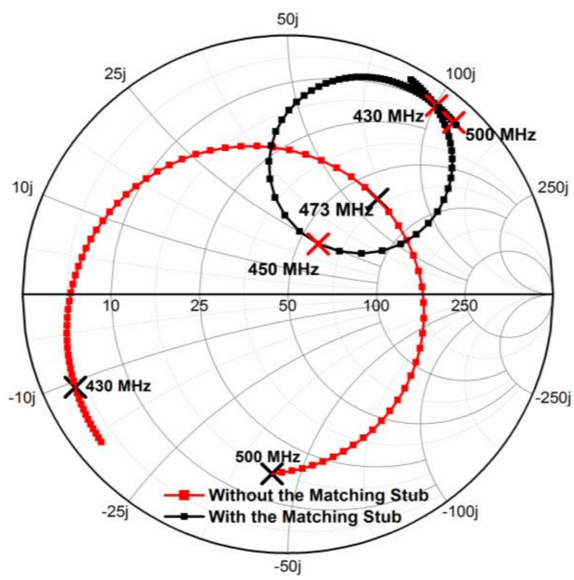

Fig. 2. Smith Chart (Simulated results).

The key advantage of the rear feeding and grounding position is to allow more freedom of available space for the meander-line and to confine the electrical length into a compact physical size.

The position of the via-slider for resonance at 450 MHz is P = 17 mm with a -10 dB impedance bandwidth of 7.2 MHz (446.5–453.7 MHz) and a -6 dB impedance bandwidth of 12.6 MHz (444.1–456.7 MHz).

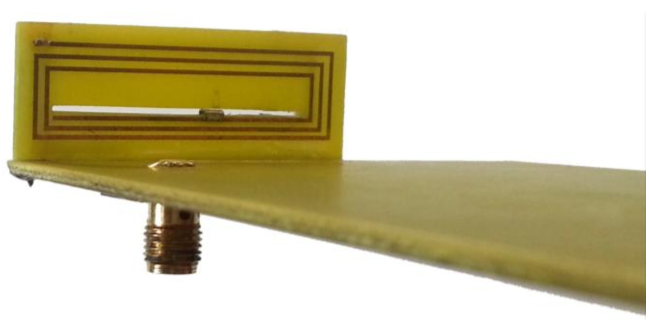

Fig. 3. Illustration of the meandered folded monopole antenna prototype.

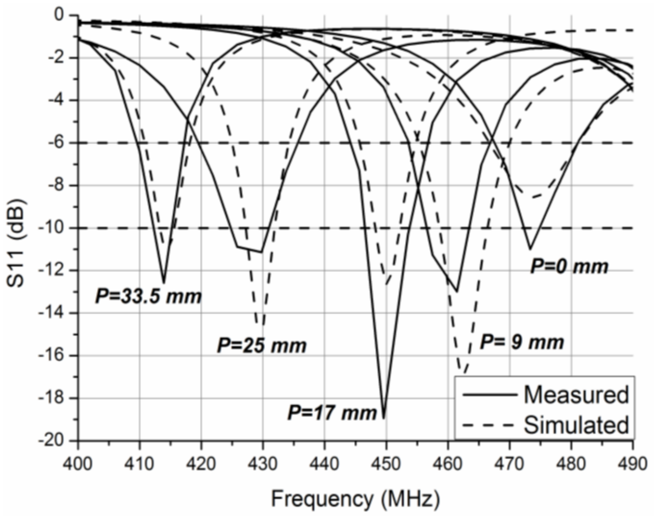

Fig. 4. Simulated and measured S_{11} results.

Fig. 5 shows the variation of S_{11} as a function of ground plane size. From the graph it is clearly visible that the size of the ground plane does not significantly affect the resonant frequency and the impedance matching of the antenna. Hence the performance of the antenna is not heavily dependent on the ground plane size.

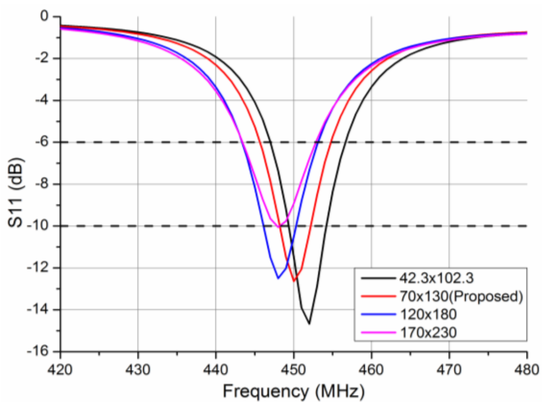

Fig. 5. The simulated S_{11} dependence on the size of the ground plane.

The total efficiency was measured in a 12 meter ETS Lindgren tapered anechoic chamber by Taoglas Ltd. and is illustrated in Fig. 6 for three different via-slider positions and indicates 21% total efficiency at 420 MHz, 24% at 450 MHz and 21.7% at 470 MHz.

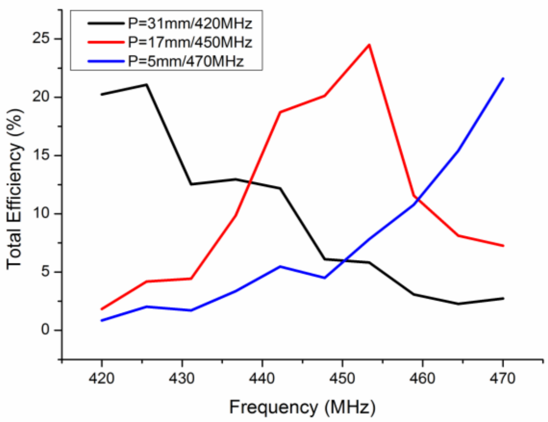

Fig. 6. Total measured efficiency of the antenna for various slider positions *P*.

In Figs. 7-9 the measured and simulated azimuth (x–z) and elevation (x–y) and (y–z) plane radiation patterns at 450 MHz are illustrated. The maximum measured gain is -6.1 dBi. There is good agreement between the measured and the simulated results. The radiation patterns are stable across the tunable band.

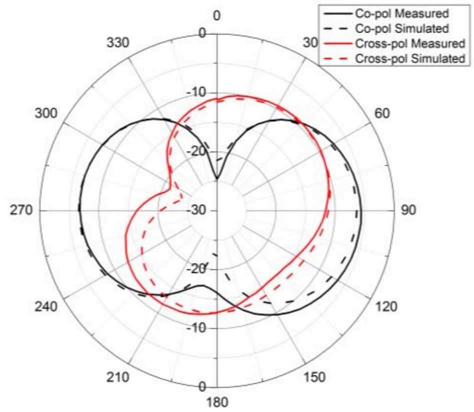

Fig. 7. Azimuth radiation patterns in the xy-plane at 450 MHz.

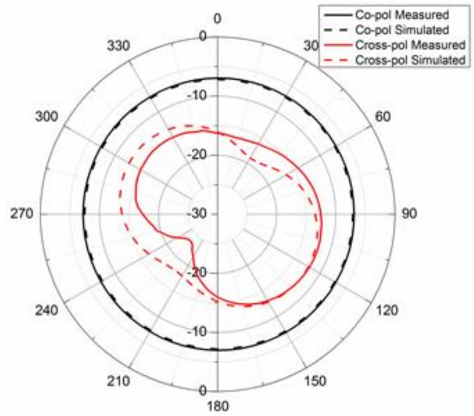

Fig. 8. Elevation radiation patterns in the xz-plane at 450 MHz.

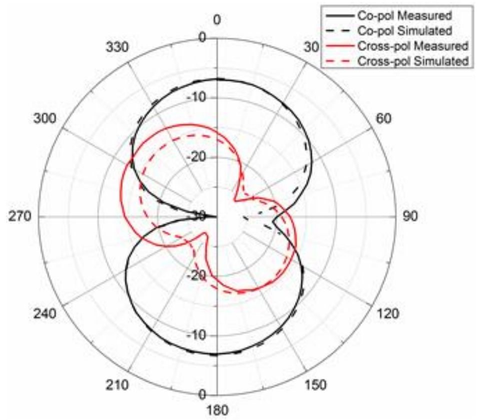

Fig. 9. Elevation radiation patterns in the yz-plane at 450 MHz.

IV. Installed Performance

To investigate the installed performance of the proposed antenna, a simulation model was created (Fig. 10) with the antenna located on a 130 mm × 70 mm ground plane size in a Plexiglas housing ($\varepsilon_r = 3.6$, $\tan\delta = 0.001$ and wall thickness = 3 mm) with outer dimensions of 81 × 266 × 172 mm^3 (H × L × W) and placed on a concrete wall ($\varepsilon_r = 5.8$ at 450 MHz, thickness = 200 mm).

Two scenarios were evaluated, with the antenna ground plane oriented parallel and perpendicular to the wall surface as shown in the Fig. 10.

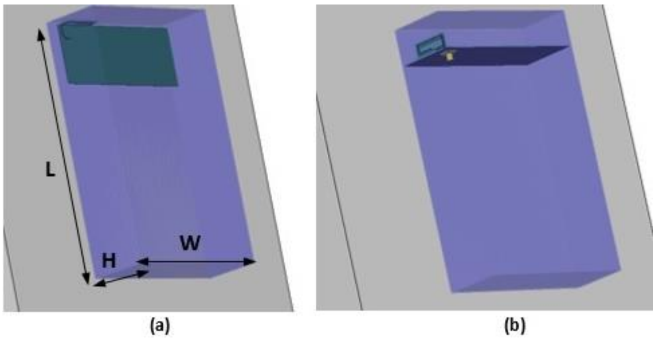

Fig. 10. The simulation model with the antenna ground plane (a) parallel to the wall and (b) perpendicular to the wall.

Figs. 11 and 12 show the measured and simulated S_{11} for the two different orientations. From inspection of the results, the resonant frequency shifts downwards due to the wall permittivity loading and this becomes more acute when the monopole is closer to the wall surface (parallel case). The distance between the edge of the ground plane and the wall for the parallel and perpendicular case was respectively 13.1 mm and 3.5 mm. For the parallel case the resonant frequency shifted downwards by 8 MHz for simulation and by 9 MHz measured. For the perpendicular case the frequency shifted downwards by 7 MHz for simulation and by 7.5 MHz for the measured case.

To mitigate the wall loading detuning effects, the slider was adjusted to tune the antenna back to 450 MHz. This also improved the total efficiency for both cases. The simulated total efficiency for the parallel case before retuning was 17.6% and after retuning was 22.9%. For the perpendicular case the simulated total efficiency before retuning was 14.5% and after was 19.7%. In both cases some energy is absorbed by the concrete wall. This absorption is greater for the perpendicular case where the total efficiency is 3.2 percentage points less than for the parallel case. For both cases the via-slider was re-adjusted to tune the resonant frequency to 450 MHz. The via-slider positions were $P = 21.3$ mm and $P = 20.3$ mm for the parallel and perpendicular cases respectively.

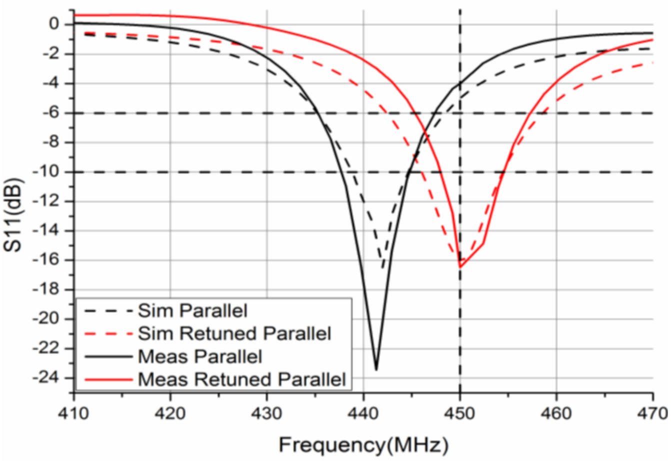

Fig. 11. Simulated and measured S_{11} for the parallel case.

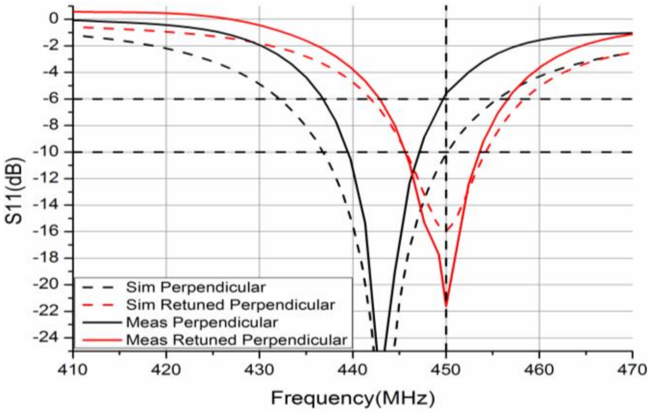

Fig. 12. Simulated and measured S_{11} for the perpendicular case.

V. Conclusions

A meander-line folded monopole antenna for emerging applications in smart metering at 450 MHz was presented. The low-cost antenna is easily fabricated with a sliding via for tuning providing the lower UHF band (412–475 MHz). The proposed compact antenna had stable omnidirectional radiation patterns across the tuneable band. With at least 21% measured total-efficiency; the tuned bandwidths met the channel requirements. The S_{11} characteristic was not impaired with the small sized ground plane. The packaged antenna performed well despite material loading and when installed on a concrete wall.

Acknowledgment

The authors would like to thank Taoglas Ltd. for the use of their anechoic chamber.

References

[1] CDG 450 Connectivity Special Interest Group (450SIG) White paper: The 450 MHz Band for the Smart Grid and Smart Metering, https://www.cdg.org/resources/files/white_papers/CDG450SICDG450SIG_450MHz_Band_Smart_Grid_Smart_Metering_Concept-SEPT2013.pdf. accessed August 2014

[2] Fadlullah, Z.M., Fouda, M.M., Kato, N., Takeuchi, A., Iwasaki, N., Nozaki, Y..: ‘Toward intelligent machine-to-machine communications in smart grid’, *IEEE Communications Magazine*, 49, (4), 2011, pp. 60-65.

[3] Electronic Communications Committee (ECC) Report 39: The technical impact of introducing CDMA-PAMR on 12.5 / 25 kHz PMR/PAMR technologies in the 410-430 and 450-470 MHz bands.

[4] Sooliarn Ooi, Boon Ping Koh, Grosman, O. ‘Dual Band UHF-GPS Folded Monopole Antenna’, *IEEE Antennas and Propagation Society International Symposium*, 2007, pp. 1237-1240.

[5] Sooliam Ooi, Boon Ping Koh, ‘Single-fed Dual Band UHF-GPS Helical Antenna,’ *IEEE International Workshop on Antenna Technology (IWAT)* 2006, March 2006, pp 184-187.

[6] Niamien, M. A. C., Sharaiha, A., Collardey, S. Mahdjoubi, K., ‘An electrically small frequency reconfigurable antenna for DVB-H’, *IEEE International Workshop on Antenna Technology (IWAT)*, pp. 245-248, March 2012.

[7] Canneva, F., Ferrero, F., Ribero, J., Staraj, R., ‘New Reconfigurable Small Antenna for DVB-H and GPS Standard’, *IEEE International Symposium on Antennas and Propagation (APSURSI)*, 2011, pp. 1549-1552.

[8] P. Queffelec, J. F. Pintos, A. Louzir, P. Minard, J. Perraudeau, J. L. Mattei, and D. Souriou, ‘Ultra-miniature UHF antenna using magneto dielectric material’, *ANTEM-AMEREM*, 2010, pp. 1-4.

[9] F. Ferrero, A. Chevalier, J. M. Ribero, R. Staraj, J.L. Mattei, Y. Queffelec, ‘A New Magneto-Dielectric Material Loaded, Tunable UHF Antenna for Handheld Devices’, *IEEE Antennas and Wireless Propag. Letters*, vol. 10, pp. 951-954, Sep. 2011.

[10] Buckley, J., Gaetano, D., McCarthy, K.G., Loizou, L., O'Flynn, B., O'Mathuna, C., ‘Compact 433 MHz antenna for wireless smart system applications’, Electronic Letters, vol. 50, (8) pp. 572-574, 2014.